Archives of Insect Biochemistry and Physiology 61:77–86 (2006)

Structure and Enzyme Properties of *Zabrotes subfasciatus* α-Amylase

Patrícia B. Pelegrini,[1] André M. Murad,[1] Maria F. Grossi-de-Sá,[2] Luciane V. Mello,[2] Luiz A.S. Romeiro,[3] Eliane F. Noronha,[1] Ruy A. Caldas,[1] and Octávio L. Franco[1]*

Digestive α-amylases play an essential role in insect carbohydrate metabolism. These enzymes belong to an endo-type group. They catalyse starch hydrolysis, and are involved in energy production. Larvae of *Zabrotes subfasciatus*, the Mexican bean weevil, are able to infest stored common beans *Phaseolus vulgaris*, causing severe crop losses in Latin America and Africa. Their α-amylase (ZSA) is a well-studied but not completely understood enzyme, having specific characteristics when compared to other insect α-amylases. This report provides more knowledge about its chemical nature, including a description of its optimum pH (6.0 to 7.0) and temperature (20–30°C). Furthermore, ion effects on ZSA activity were also determined, showing that three divalent ions (Mn^{2+}, Ca^{2+}, and Ba^{2+}) were able to enhance starch hydrolysis. Fe^{2+} appeared to decrease α-amylase activity by half. ZSA kinetic parameters were also determined and compared to other insect α-amylases. A three-dimensional model is proposed in order to indicate probable residues involved in catalysis (Asp_{204}, Glu_{240}, and Asp_{305}) as well other important residues related to starch binding (His_{118}, Ala_{206}, Lys_{207}, and His_{304}). Arch. Insect Biochem. Physiol. 61:77–86, 2006.

KEYWORDS: *Zabrotes subfasciatus*; α-amylase; molecular modelling; enzyme activity; bean bruchid

INTRODUCTION

Phaseolus vulgaris is an important legume for human diet as well for many other animals, since it is an important energy source. This crop provides income for farmers due to a brief life cycle, producing two or three crops a year (Mbithi-Mwikya et al., 2002). In general, bean crop losses caused by insect pests reach 13–25% (Schroeder et al., 1995; Morton et al., 2000). Among different Coleopterans that attack *P. vulgaris*, storage pests are economically important, since they cause severe damage to seed and seedpods. These bruchids, such as the common bean weevil *Acanthoscelides obtectus* and the Mexican bean weevil *Zabrotes subfasciatus*, feed on grains causing reduction of nutritional quality and germination power, leading to economic losses to producers and consumers (Macedo et al., 2002). Potential losses are attenuated, however, because plants have a certain degree of insect resistance, as observed in several studies describing defensive chemical compounds biosynthesised in plants (Franco et al., 2002; Payan, 2004; Haq et al., 2004).

[1]Centro de Análises Proteômicas e Bioquímica, Programa de Pós-Graduação em Ciências Genômicas e Biotecnologia, Universidade Católica de Brasilia, Brasília-DF, Brazil

[2]Embrapa, Cenargen, Brasília-DF, Brazil

[3]Curso de Química, Universidade Católica de Brasília, Brasília-DF, Brazil

Contract grant sponsor: Universidade Catolica de Brasilia; Contract grant sponsor: CNPq; Contract grant sponsor: CAPES; Contract grant sponsor: EMBRAPA.

Abbreviations used: α-AI2 = *Phaseolus vulgaris* α-amylase inhibitor variant II; DMSO = dymethylsulphoxide; PDB = Protein Data Bank; PVP = polyvinylpyrrolidone; SDS-PAGE = sodium dodecyl sulphate polyacrilamide gel electrophoresis; TMA = *Tenebrio molitor* α-amylase; ZSA = *Zabrotes subfasciatus* α-amylase; 3.5 DNS = 3.5 dinitrosalicylic sulphate.

*Correspondence to: Octávio L. Franco, SGAN Quadra 916, Módulo B, Av. W5 Norte 70.790-160, Asa Norte, Brasília, DF-Brazil. E-mail: ocfranco@pos.ucb.br

Received 5 April 2005; Accepted 5 August 2005

DOI: 10.1002/arch.20099
Published online in Wiley InterScience (www.interscience.wiley.com)

P. vulgaris seeds are rich sources of starch (Sehnke et al., 2000; Pilling and Smith, 2003). This compound is characterized by glucose polymers linked together by α-1.4 and α-1.6 glycosidic bonds (Nelson and Cox, 2000). Several insect pests, especially those that feed on starchy grains during larval and/or adult life such as the Mexican bean weevil, depend on their α-amylases for survival. Among them, *Z. subfasciatus* α-amylase (ZSA) is a well-studied but not completely understood enzyme (Grossi-de-Sá and Chrispeels, 1997). The ZSA primary structure predicts a protein with 483 amino acid residues, which exhibits similarity to other insect and mammalian α-amylases (Grossi-de-Sá and Chrispeels, 1997). Although several inhibitors have been tested against ZSA, including α-AI2 from bean seeds (Grossi-de-Sá and Chrispeels, 1997) and cereal-like inhibitors from wheat kernels (Franco et al., 2000), none are effective in the control of *Z. subfasciatus*. This report focuses the elucidation of additional biochemical properties of ZSA. Temperature and pH optima, as well as the effects of ions, were analysed in detail. Additionally, kinetic parameters were determined and a three-dimensional model was constructed to elucidate the tertiary structure of ZSA and the possible residues involved in catalytic activity.

MATERIALS AND METHODS

Insects

Z. subfasciatus larvae were obtained from Plant-Pest Interaction Laboratory (Embrapa-Cenargen, Brasília, Brazil). The larvae were reared at 24°C in a relative humidity of 70 ± 10% and a 12-h photoperiod. The insects were routinely maintained on common bean (*P. vulgaris*) seeds.

Z. subfasciatus α-Amylase Expression

The full-length ZSA cDNA was subcloned in pBacPak1 (Clontech, Palo Alto, CA) vector and *Spodoptera frugiperda* SF9 cells were used for the expression as described by Grossi-de-Sá and Chrispeels (1997). Cells were cultured at 28°C in Grace's medium (GibcoBRL, Gaithersburg, MD) supplemented with 10% fetal calf serum (GibcoBRL) and 50 $\mu g.ml^{-1}$ gentamicin. For transfection of cells, 2.5 μg of transfer vector containing the target gene and 0.25 μg BaculoGoild™ virus DNA (PharMingen, San Diego, CA) were co-transfected into 1×10^6 Sf9 cells plated with 0.7 ml of Grace's medium in a 35-mm tissue culture dish by the lipofection method. Cells were incubated with the liposome-DNA complexes for 5 h and then were re-fed with 2.5 ml of Grace's media containing 10% fetal calf serum. After 72 h, the medium that contained the viruses produced by the transfected cells was transferred to a sterile tube and stored at 4°C. Sf9 monolayers were reinfected with the recombinant baculovirus inocula supernatant. Approximately 2.5×10^6 cells in 5 ml of Grace's-10% fetal calf serum were infected with 5 $pfu.cell^{-1}$ of recombinant baculovirus. The infected cells were cultured for 72 h before harvest following sedimentation of cells by centrifugation for 10 min at 1,000*g*. The cells were lysed for 45 min on ice in lysis buffer (10 mM Tris-HCl pH 7.5, 130 mM NaCl, 1% Triton, X-100, 10 mM NaF, 10 mM sodium phosphate, and 10 mM sodium pyrophosphate) containing a protease inhibitor cocktail (800 $\mu g.ml^{-1}$ benzamidine HCl, 500 $\mu g.ml^{-1}$, phenanthroline, 500 $\mu g.ml^{-1}$ aprotinin, 500 $\mu g.ml^{-1}$ leupeptin, 500 $\mu g.ml^{-1}$ pepstatin A, and 50 mM phenylmethylsulfonyl fluoride). Lysate was clarified by centrifugation at 10,000*g* for 30 min to pellet the cellular debris.

Z. subfasciatus α-Amylase Purification

Lysate was applied onto an affinity chromatography Sepharose-6B conjugated with β-cyclodextrin equilibrated with 0.1 M phosphate buffer, pH 5.8, containing 20 mM NaCl and 0.1 mM $CaCl_2$. The adsorbed proteins were eluted with one single step of 20 mM β-cyclodextrin. Fractions (2.0 ml) were collected at a flow rate of 28 $ml.h^{-1}$ and used to measure α-amylolytic activity. Retained fractions were pooled, dialyzed for 48 h against distilled water, and concentrated. Purified ZSA was analysed by SDS-PAGE mini-gels 15% at a standard concentration of 10 $\mu g.ml^{-1}$ according Laemmli (1970).

Enzymatic Assays

α-Amylase activities were measured according to Bernfeld (1955), using five enzyme concentrations (6.25, 12.5, 25.0, 50.0, and 100.0 $\mu g.ml^{-1}$) diluted in sodium acetate buffer 0.05 M, pH 6.0; 1% starch was added to the reaction as substrate; each fraction was incubated at 37°C for 20 min. Enzymatic reaction was stopped by adding 1.0 ml of 3.5 DNS (1% dinitrosalicylic acid dissolved in 0.2 M NaOH and 30% sodium potassium tartrate) and was evaluated by optical density at 530 nm. Each assay was carried out in triplicate.

Biochemical Characterization of *Z. subfasciatus* α-Amylase (ZSA)

All ZSA biochemical properties were determined using enzyme at a standard concentration of 20 $\mu g.ml^{-1}$ diluted in 0.05 M acetate buffer, pH 6.5, containing 0.05 M $CaCl_2$. Each fraction was pre-incubated for 10 min at different temperatures from 0 to 100°C (varying by 10°C). The ZSA pH optimum was determined, pre-incubating amylase at a range of pH 3.0 to 8.0 for 10 min at 37°C, using a 0.05 M sodium acetate buffer containing 10 mM NaCl and 5 mM $CaCl_2$, pH 6.5. After pre-incubation enzyme activity, optima pH and temperature were obtained by determination of optical density lectures at 530 nm. Each assay was carried out in triplicate. Denaturation analysis was done pre-incubating ZSA for 10 min at different temperatures from 0 to 100°C (varying by 10°C). Evaluation of ZSA stability was obtained by optical density analysis at 280 nm.

Enzyme activities were determined and compared using twelve ions and other compounds, such as 10 $\mu g.ml^{-1}$ $FeCl_2$, 10 $\mu g.ml^{-1}$ $NiCl_2$, 10 $\mu g.ml^{-1}$ $MgCl_2$, 10 $\mu g.ml^{-1}$ $MnCl_2$, 10 $\mu g.ml^{-1}$ glycine, 10 $\mu g.ml^{-1}$ urea, 10 $\mu g.ml^{-1}$ $Ba(C_2O_3H_2)_2$, 10 $\mu g.ml^{-1}$ phenol, 10 $\mu g.ml^{-1}$ glycerol, and 10 $\mu g.ml^{-1}$ $Ca(C_2O_3H_2)_2$. Also used were 7 $\mu g.ml^{-1}$ $LiSO_4$ and 7$\mu g.ml^{-1}$ polyvinylpyrrolidone (PVP). The reaction mixtures (compound, enzyme, and buffer) were pre-incubated for 20 min, and assays were carried out as described before.

Statistical analyses were carried out using a completely random design and the comparisons of the means of the treatments were made by Tukey's test at a 5% level of probability.

Kinetic Parameters of ZSA

Kinetic parameters of ZSA were determined for soluble starch according to Yang et al. (2004). Samples (50 µl) from reaction mixture containing ZSA and also substrate dissolved in 50 mM sodium acetate buffer (pH 6.0) at 37°C were taken at intervals of 90 s, and then reaction was immediately stopped by adding dinitrosalicylic acid and boiling as described. The amount of reducing sugars produced from soluble starch was measured according Bernfeld (1955). Kinetic data were transformed to Lineweaver-Burk plots and Km values were calculated from the slopes of the curves.

Model Construction

The 483 ZSA residues sequence was obtained from NCBI (code AAF73435) and an alignment against PDB structures was done in order to find a specific template. For this purpose, the BioInfo Meta Server (Ginalski et al., 2003) was used and the best scores of FFAS03 (129) and ORFeus-2 (351) indicated that *Tenebrio molitor* α-amylase (TMA) (Strobl et al., 1998a) structure (PDB code: 1clv) showed an enhanced structural similarity. The model was constructed using DeepView/Swiss PdbViewer Program, version 3.7, developed by the Swiss Institute of Bioinformatics (Guex and Peitsch, 1997). A raw sequence of ZSA was loaded and fitted according to structural alignment produced before. After superposition of atomic coordinates of 471 residues, an energy minimization was done using Gromos96, a force field that predicts the dependence of a molecular conformation on the type of environment (water, methanol, chloroform, DMSO, non-polar solvent, crystal, etc.). The program calculates the relative binding constants by evaluating free energy differences between various molecular complexes using thermodynamic integration, perturbation, and extrapolation. The pro-

gram predicts energetic and structural changes caused by modification of amino acids in enzymes. This method used six subsequent rounds, minimizing backbone and side chains (88,000 steps of steepest descent and 44,000 steps of conjugate gradients). It was also necessary to reconstruct peptide bonds between Asn_{358}, Ile_{359}, Cys_{360}, Tyr_{228}, and Phe_{229}. Ramachandran plot and rmsd values were considered to validate the model.

RESULTS

Biochemical Characterization of *Z. subfasciatus* α-Amylase

Aiming to understand *Z. subfasciatus* starch digestion, ZSA was expressed in insect cells, extracted, and loaded onto an Epoxi-Sepharose 6B affinity (Fig. 1A). Adsorbed material was eluted using a single step of β-cyclodextrin. Silver stained SDS-PAGE analysis showed a single band of approximately 47.0 kDa. Enzymatic assays using purified ZSA were carried out in order to determinate biochemical properties. A thermostability curve was constructed, showing higher α-amylolytic activity between 20° and 30°C (Fig. 2A). The enzyme maintained its stability up to 60°C, after which there was a pronounced activity reduction. Comparing both graphs from UV 280 nm and visible 530 nm (Fig. 2A and B), a unique convergence point occurred at 70°C, where enzyme activity decreased and UV absorbance increased. Enzyme denaturation was indicated by optical density at 280 nm.

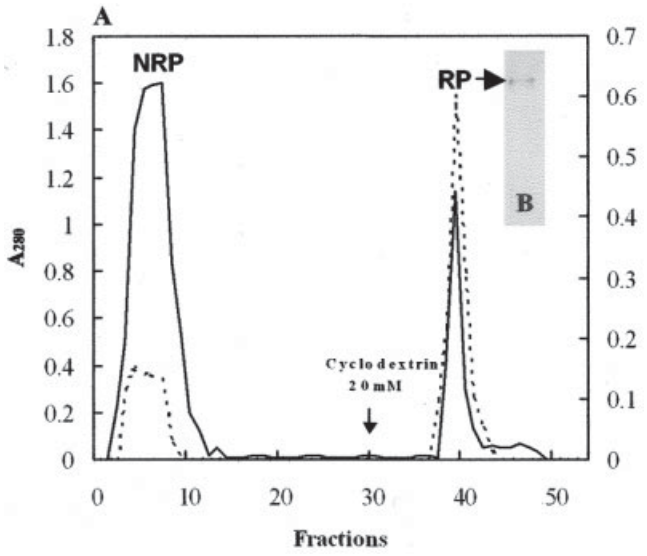

Fig. 1. Purification of α-amylase from *Z. subfasciatus*. Chromatographic profile obtained (A) during the Epoxi-Sepharose 6B chromatography equilibrated with 0.1 M phosphate buffer, pH 5.8, containing 20 mM NaCl and 0.1 mM $CaCl_2$. The black arrow indicates the single step application of 20 mM β-cyclodextrin dissolved in the same buffer. Dashed line indicates α-amylolytic activity. The material eluted in individual peaks was collected, lyophilised, and stored at –20°C. **B:** SDS-PAGE 15% analysis of purified ZSA stained with silver.

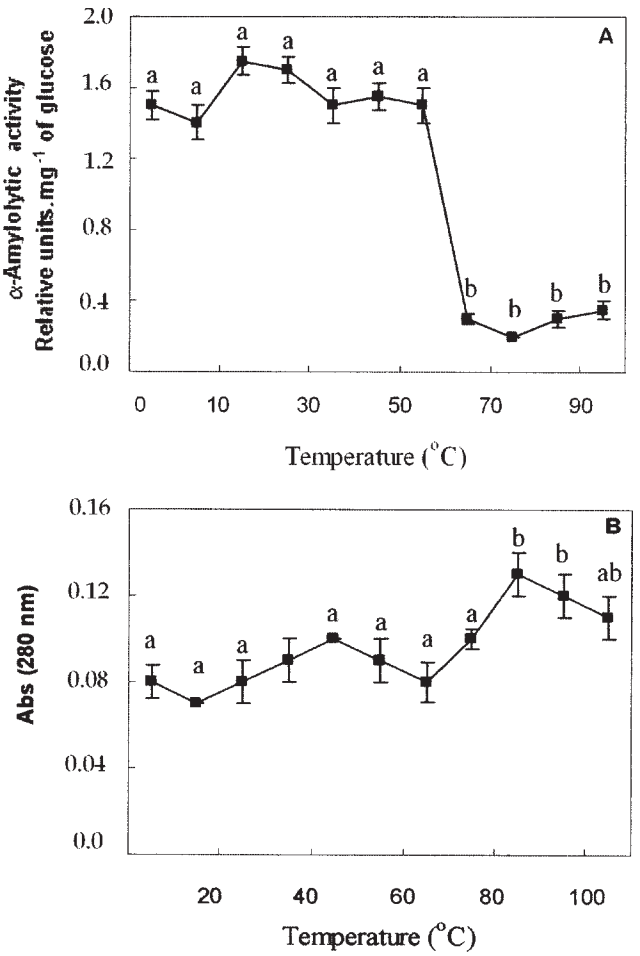

Fig. 2. Temperature effects on ZSA α-amylolytic activity (A) and structure stability (B). Each assay was done in triplicate and vertical bars correspond to standard deviation. Mean values followed by the same letter were not statistically different ($P < 0.05$) by Tukey's test.

Since aromatic residues exposition was analysed, the evaluation of absorbances varied between 0° and 50°C, and just after 60°C, the UV absorbance increased, indicating a probable enzyme denaturation. A broad pH optimum between 6.0 and 7.0 was observed (Fig. 3A). Lower activity occurred at acidic pHs (3.0 to 5.0). ZSA stability was enhanced in the presence of ion calcium, especially between pH 6.0 and 8.0 (Fig. 3B).

α-Amylases utilize several compounds and ions that stabilize the enzyme structure (Haddaoui et al., 1997; Ilori et al., 1997; Valencia et al., 2000). In this report, ZSA activity was assayed in the presence of ions and organic compounds [$FeCl_2$, $NiCl_2$, $MgCl_2$, $MnCl_2$, Li_2SO_4, glycine, urea, $Ba(C_2H_3O_2)_2$, polyvinylpyrrolidone, phenol, glycerol, and $Ca(C_2H_3O_2)_2$]. All substances enhanced enzyme activity with exception of $FeCl_2$. $MnCl_2$ caused a remarkable increase in ZSA activity, followed by $Ba(C_2H_3O_2)_2$ and urea (Fig. 4). Li_2SO_4 similarly enhanced the enzyme activity followed by phenol, $NiCl_2$, $Ca(C_2H_3O_2)_2$, PVP, glycine, $MgCl_2$, and glycerol (Fig. 4). The values observed for this test did not differ more than 12% for each substance tested, as evaluated by Tukey's test. Kinetic parameters obtained by a Lineweaver-Burk plot showed a Km of 0.013 mM (data not shown), indicating that starch is a favourable substrate for ZSA demonstrating the ability to hydrolyse starch in a highly specific interaction enzyme-substrate.

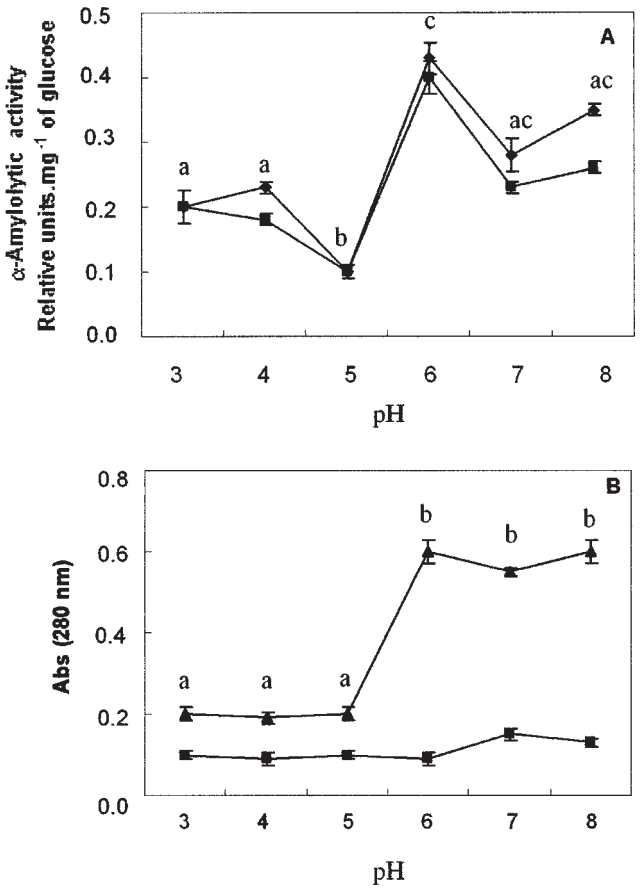

Fig. 3. pH effects on ZSA α-amylolytic activity (A) and structure stability (B) in the absence (■) and presence (▲) of 50 mM calcium chloride. Each assay was done in triplicate and vertical bars correspond to standard deviation. Mean values followed by the same letter were not statistically different ($P < 0.05$) by Tukey's test.

Theoretical Characterization of ZSA

Structural alignment against other α-amylases indicated high residue conservation involved in the catalytic process and also conserved residues in the adjacent site (Fig. 5). This alignment showed that three domains (A, B, and C) formed ZSA. This

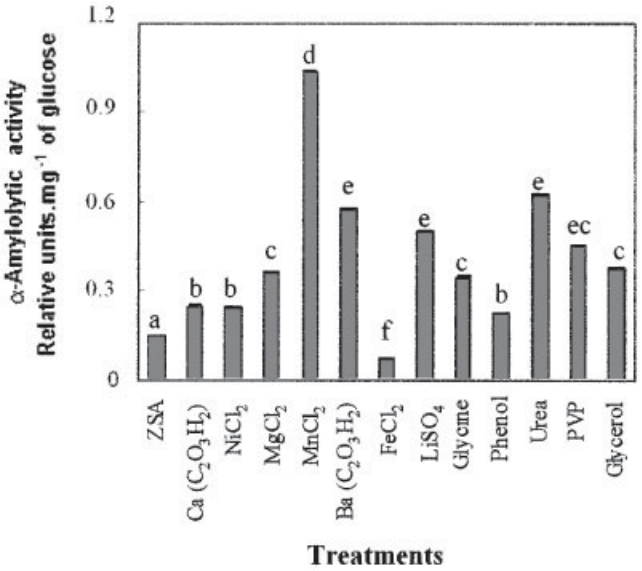

Fig. 4. Ionic and organic compounds effects on ZSA α-amylolytic activity. Each assay was done in triplicate and each replicate does not differ more than 10%. Mean values followed by the same letter were not statistically different ($P < 0.05$) by Tukey's test.

Fig. 5. Structural alignment of *Z. subfasciatus* α-amylase (ZSA) and primary structure of *T. molitor* α-amylase (TMA-PDB: 1tmq). Catalytic triad residues are in bold and italic and basic residues involved in starch orientation are only in bold. Secondary structures are represented by grey arrows in β-sheets and grey cylinders for α-helices.

could be easily recognized (Fig. 6), as compared to TMA three-dimensional structure (Strobl et al., 1998a). Domain B is a deformed β-sheet, while the C domain is formed by a set of β-sheets and the A domain is structured in a $(\alpha/\beta)_8$ barrel. Furthermore, possible α-amylase residues involved in catalysis (Asp_{204}, Glu_{240}, and Asp_{305}) are extremely conserved, forming the catalytic triad of active site as well as the basic residues involved in orientation of starch molecules (His_{118}, Ala_{206}, Lys_{207}, and His_{304}) (Figs. 5 and 6). In a Ramachandran plot analysis, only 2.5% of residues were in disallowed regions. Further analysis of dynamics could suggest different conformational changes.

DISCUSSION

Several practical and theoretical properties were determined for ZSA. In this report, we have found that at 20° and 30°C, the enzyme showed higher activity, while at 60°C, ZSA activity decreased. This effect probably was caused by a thermal denaturation, which was observed at 280 nm. Probably, ZSA denaturation could occur due to surface exposition of hydrophobic residues involved on α-amylase stabilization, as tryptophan and phenylalanine. The *T. molitor* and *D. melanogaster* α-amylases presented optima temperature for its activity at 37°C, similar to ZSA thermostability (Buonocore et al., 1976; Shibata and Yamazaki, 1994).

Since ZSA pH optimum was around 6.0, similar results were also found in β-amylases from germinating millet *P. miliaceum*, which showed higher stability in a pH range of 5.5 to 6.0 (Yamasaki, 2003). Furthermore, the barley α-amylase (AMY2) showed enhanced activity at pH 7.4 (Nielsen et al., 2004). An optimum pH, between 6.0 and 7.0, was also found in several insect midgut pH, such as *T. molitor*, *H. hampei*, and *C. maculatus* (Valencia et al., 2000; Franco et al., 2002), suggesting that

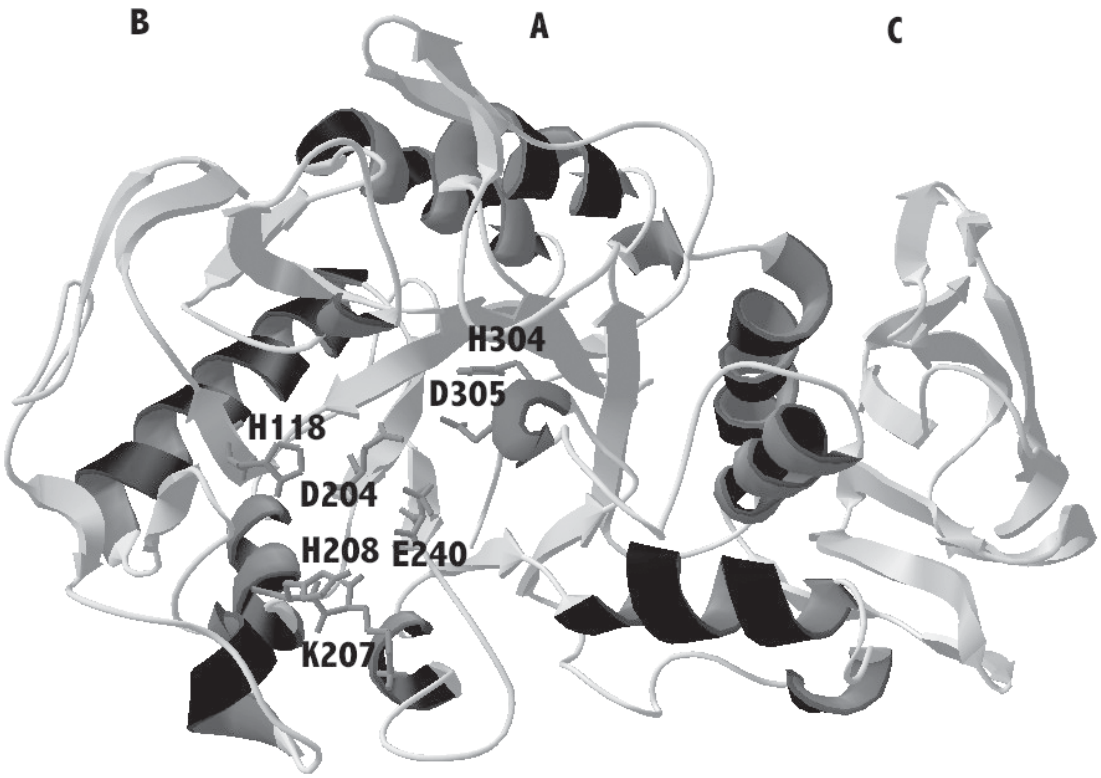

Fig. 6. Ribbon structure of a three-dimensional model of *Z. subfasciatus* α-amylase. A, B, and C indicate the α-amylase domains; dark grey arrows indicate β-sheets; and light grey colour indicates α-helices. The catalytic site is also focused. Possible residues involved in enzymatic catalysis and their respective side chains are shown in black (Asp204, Asp305, and Glu240). Indicated positive charged side chain residues H304, H208, H118, and K207 probably are involved in binding and stabilization of substrate.

α-amylases from those insect-pests might behave similarly to ZSA. The presence of calcium chloride increased ZSA stability, especially at pH between 6.0 and 8.0. ZSA optimum pH for its activity is similar to that found previously for α-amylase inhibition by αAI-1 and αAI-2 (Grossi-de-Sá and Chrispeels, 1997) indicating that at this pH, several inhibitors could show efficiency toward this target α-amylase.

ZSA activity was assayed in the presence of several compounds, since some enzymes require at least one calcium ion for catalytic activity and sometimes another ion to prevent its destruction in the human gut by proteolytical enzymes (Strobl et al., 1998a; Xavier-Filho et al., 1999; Valencia et al., 2000). This could explain the results obtained for Ca $(C_2H_3O_2)_2$ and $MnCl_2$, where low concentrations stabilized the enzyme and cause a remarkable increase in ZSA activity. Urea and $Ba(C_2H_3O_2)_2$ provided a similar response to enzymatic activity, increasing it. Barium ion is associated with *Bacillus subtilis* α-amylase stability and activity (Haddaoui et al., 1997). However, further studies might be done to understand the biochemical mechanisms of why urea increased ZSA activity.

Reactions in the presence of $MnCl_2$ yielded the highest increase in ZSA activity. There have not been earlier reports describing the influence of manganese ion on α-amylase activity. Reactions in the presence of $MgCl_2$ also yielded an increase in ZSA activity. Magnesium ions could increase α-amylase activity in bacteria (Ilori et al., 1997). Therefore, in the presence of two stimulating ions, magnesium and chloride, ZSA activity was increased more than reactions in the presence of calcium. Glycine may also enhance enzyme activity, but at a lower level

compared to results with substances reported here (Rendleman, 2000). $NiCl_2$ also stimulated ZSA activity, although it is not well understood how nickel can influence starch hydrolysis. α-Amylase probably had its activity increased by an ion replacement, as observed by Wiegand et al. (1995). Glycine, PVP, and glycerol also increased ZSA activity. Glycine is related to a long-term stability of α-amylases (Wang et al., 2004). Glycerol did not increase activity of α-amylase from *Bacillus licheniformis* (Esteve-Romero et al., 1996). Moreover, reactions with polyvinylpyrrolidone did not influence enzyme activity or stability for human salivary and pancreatic α-amylase, and also for porcine pancreatic α-amylase (Bretaudiere et al., 1981). For β-amylase, in contrast to α-amylase, magnesium, calcium, and zinc ions decreased the enzyme activity (Dahot et al., 2004). Probably, ions act differently on β-amylases in comparison to α-amylases, due to differences in primary structure and catalytic sites.

Reactions in the presence of $FeCl_2$ decreased ZSA activity. Rat, mice, and human α-amylase activity was reduced in a high iron concentration in the serum (Teotia and Gupta, 2001). The activity of β-amylase from *P. miliaceum*, was inhibited by divalent ions such as Hg^{2+}, Mn^{2+}, and Cu^{2+} (Yamasaki, 2003). There are several inhibition mechanisms proposed, including binding between inhibitor and enzyme (Bompard-Gilles et al., 1996; Strobl et al., 1998b) or by ion chelation (Franco et al., 2002). It seems that $FeCl_2$ inhibits enzyme activity by calcium replacement as observed in α-amylases from mammalian serum (Yamasaki, 2003).

Kinetic parameters showed a Km of 0.013 mM for ZSA, when expressed in percentage of substrate (starch) in solution. As Km value indicates enzyme-substrate specificity, it seems that ZSA demonstrates high interaction with starch. This result is similar to other insect α-amylases, such as those from *Drosophila* species, where Km values were between 0.063 and 0.081 (Prigent et al., 1998). Otherwise, a thermostable α-amylase from *Pyrococcus furiosus* revealed a Km value of 0.52 mM for starch (Yang et al., 2004).

The proposed ZSA model showed structural similarities with other well-characterized α-amylases, such as porcine pancreatic α-amylase (Payan and Qian, 2003) and *Alteromonas haloplancti* (Aghajari et al., 1998). A, B, and C domains encountered in α-amylases could be recognized. The catalytic triad position, located in the bottom of the $(\alpha/\beta)_8$ barrel, is extremely conserved in both enzymes (ZSA and TMA), as are the residues involved in substrate orientation. In a comparison of sequence homology and structure of other α-amylases, it can be suggested that they share a common catalytic mechanism, so it is possible that A and B ZSA domains can accommodate at least six sugar units, and the hydrolyses may occur between the third and the fourth pyranose (Machius et al., 1996; Strobl et al., 1998a; Franco et al., 2002). On the basis of three acidic residues, the mechanism of catalysis involves a nucleophilic attack of a water molecule on C_1 of subsite 3 of moiety sugar bond resulting in a linearization of pyranose, followed by the hydrolyse of the chain. Our ZSA model needs the same ions for orientation and binding to a starch molecule. Disulfide bonds of the model also need special attention in order to investigate the structural stability in spite of having one less bond than TMA. Despite temperature and pressure stability, the ZSA has nine cysteine residues and three disulfide bonds (Cys_{445}-Cys_{433}, Cys_{43}-Cys_{103}, and Cys_{153}-Cys_{167}). This indicates that ZSA could be unstable when compared to TMA, which has 15 cysteine residues and seven disulfide bonds (Cys_{134}-Cys_{138}, Cys_{518}-Cys_{501}, Cys_{517}-Cys_{531}, Cys_{508}-Cys_{523}, Cys_{360}-Cys_{354}, Cys_{28}-Cys_{84}, and Cys_{425}-Cys_{437}) conferring a more stable conformation. Free cysteine residues in ZSA, Cys_{368}, Cys_{360}, and Cys_{132}, are separated by an average distance of 20 Å, making impossible the formation of disulfide bonds.

ACKNOWLEDGMENTS

The authors are grateful to Dr. David Stanley for a critical reading of the paper, and to Dr. Marten Chrispeels for the use of ZSA gene.

LITERATURE CITED

Aghajari N, Feller G, Gerday C, Haser R. 1998. Crystal structures of the psychrophilic α-amylase from *Alteromonas*

haloplanctis in its native form and complexed with an inhibitor. Protein Sci 7:564.

Bernfeld P. 1955. Amylases α and β. Methods Enzymol 1:149–150.

Bompard-Gilles C, Rousseanu P, Rouge P, Payan F. 1996. Substrate mimicry in the active centre of a mammalian model of the α-amylase: structural analysis of an enzyme inhibitor complex. Structure 4:1441–1452.

Bretaudiere JP, Rej R, Drake P, Vassaault A, Bailly M. 1981. Suitability of control materials for determination of α-amylase activity. Clin Chem 27:806–815.

Buonocore V, Poerio E, Silano V, Tomasi M. 1976. Physical and catalytic properties of α-amylase from *Tenebrio molitor* L. larvae. Biochem J 153:621–625.

Dahot MU, Saboury AA, Moosavi-Movahedi AA. 2004. Inhibition of β-amylase activity by calcium, magnesium and zinc ions determined by spectrophotometry and isothermal titration calorimetry. J Enzyme Inhib Med Chem 19:157–160.

Esteve-Romero J S, Bossi A, Righetti PG. 1996. Purification of thermamylase in multicompartment electrolyzers with isoelectric membranes: the problem of protein solubility. Electrophoresis 17:1242–1247.

Franco OL, Rigden DJ, Melo FR, Bloch C Jr., Silva CP, Grossi-de-Sá MF. 2000. Activity of wheat α-amylase inhibitor towards bruchid α-amylases and structural explanation of observed specificities. Eur J Biochem 267:2166–2173.

Franco OL, Rigden DJ, Melo FR, Grossi-de-Sá MF. 2002. Plant α-amylase inhibitors and their interaction with insect α-amylases–structure, function and potential for crop protection. Eur J Biochem 269:397–412.

Ginalski K, Elofsson A, Fischer D, Rychlewski L. 2003. 3D-Jury: a simple approach to improve protein structure predictions. Bioinformatics 19:1015–1018.

Grossi-de-Sá MF, Chrispeels MJ. 1997. Molecular cloning of bruchid (*Zabrotes subfasciatus*) α-amylase cDNA and interactions of the expressed enzyme with bean amylase inhibitors. Insect Biochem Mol Biol 27:271–281.

Guex N, Peitsch MC. 1997. Swiss-model and the Swiss-PdbViewer: an environment for comparative protein modelling. Electrophoresis 18:2714–2723.

Haddaoui EA, Leloup L, Petit-Glatron MF, Chambert R. 1997. Characterization of a stable intermediate trapped during reversible refolding of *Bacillus subtilis* α-amylase. Eur J Biochem 249:505–509.

Haq SK, Atif S M, Khan RH. 2004. Protein proteinase inhibitor genes in combat against insects, pests, and pathogens: natural and engineered phytoprotection. Arch Biochem Biophys 431:145–159.

Ilori MO, Amund OO, Omidiji O. 1997. Purification and properties of an α-amylase produced by a cassava-fermenting strain of *Micrococcus luteus*. Folia Microbiol 42:445–449.

Laemmli UK. 1970. Cleavage of structural proteins during the assembly of the head of bacteriophage T4. Nature 227: 680–685.

Macedo ML, das Graças MFM, Novello JC, Marangoni S. 2002. *Talisia esculenta* lectin and larval development of *Callosobruchus maculatus* and *Zabrotes subfasciatus* (Coleoptera: Bruchidae). Biochim Biophys Acta 6:83–88.

Machius M, Vertesy L, Huber R, Wiegand G. 1996. Carbohydrate and protein-based inhibitors of porcine pancreatic α-amylase: structure analysis and comparison of their binding characteristics. J Mol Biol 260:409–421.

Mbithi-Mwikya S, Van-Camp J, Mamiro PR, Ooghe W, Kolsteren P, Huyghebaert A. 2002. Evaluation of the nutritional characteristics of a finger millet based complementary food. J Agric Food Chem 8:3030–3036.

Morton RL, Schroeder HE, Bateman KS, Chrispeels MJ, Armstrong E, Higgins TJ. 2000. Bean α-amylase inhibitor 1 in transgenic peas (*Pisum sativum*) provides complete protection from pea weevil (*Bruchus pisorum*) under field conditions. Proc Natl Acad Sci USA 97:3820–3825.

Nelson DL, Cox MM. 2000. Lehninger Principles of Biochemistry. New York: Worth Publishers, p 975.

Nielsen PK, Bonsager BC, Kukuda K, Svensson B. 2004. Barley α-amylase/subtilisin inhibitor: structure, biophysics and protein engineering. Biochim Biophys Acta 1696:157–164.

Payan F. 2004. Structural basis for the inhibition of mammalian and insect α-amylases by plant protein inhibitors. Biochim Biophys Acta 1969:171–180.

Payan F, Qian M. 2003. Crystal structure of the pig pancreatic α-amylase complexed with malto-oligosaccharides. J Prot Chem 22:275.

Pilling E, Smith AM. 2003. Growth ring formation in the starch granules of potato tubers. Plant Physiol 132:365–371.

Prigent S, Matoub M, Rouland C, Cariou M-L. 1998. Metabolic evolution in α-amylases from *Drosophila virilis* and *D. replete*, two species with different ecological niches. Comp Biochem Physiol B 119:407–412.

Rendleman JA Jr. 2000. Hydrolytic action of α-amylase on high-amylose starch of low molecular mass. Biotechnol Appl Biochem 31:171–178.

Schroeder HE, Gollasch S, Moore A, Tabe LM, Craig S, Hardie DC, Chrispeels MJ, Spencer D, Higgins T. 1995. Bean α-amylase inhibitor confers resistance to the pea weevil (*Bruchus pisorum*) in transgenic peas (*Pisum sativum* L.). Plant Physiol 107:1233–1239.

Sehnke PS, Chung H, Wu K, Ferl RJ. 2001. Regulation of starch accumulation by granule associated plant 14-3-3 proteins. Proc Natl Acad Sci USA 16:765–770.

Shibata H, Yamazaki T. 1994. A comparative study of the enzymological features of α-amylase in the *Drosophila melanogaster* species subgroup. Jpn J Genet 69:251–258.

Strobl S, Maskos K, Betz M, Wiegand G, Huber R, Gomis-Ruth FX, Glosckshuber R. 1998a. Crystal structure of yellow mealworm α-amylase at 1.64 Å resolution. J Mol Biol 278:617–628.

Strobl S, Maskos K, Wiegand G, Huber R, Gomis-Ruth FX, Glockshuber R. 1998b. A novel strategy for inhibition of α-amylases: yellow mealworm α-amylases in complex with the *Ragi* bifunctional inhibitor at 2.5 Å resolution. Structure 6:911–921.

Teotia S, Gupta MN. 2001. Purification of α-amylases using magnetic alginate beads. Appl Biochem Biotechnol 90:211–220.

Valencia A, Bustillo AE, Ossa GE, Chrispeels M J. 2000. α-Amylase of the coffee berry borer (*Hypothenemus hampei*) and their inhibition by two plant α-amylase inhibitors. Insect Biochem Mol Biol 30:207–213.

Wang DQ, Hey JM, Nail SL. 2004. Effect of collapse on the stability of freeze-dried recombinant factor VIII and α-amylase. J Pharmacol Sci 93:1253–1263.

Wiegand G, Epp O, Huber R. 1995. The crystal structure of porcine pancreatic α-amylase in complex with the microbial inhibitor Tendamistat. J Mol Biol 247:99–110.

Xavier-Filho J, Campos FAP, Silva CP, Ary MB. 1989. Resolution and partial characterization of proteinase and α-amylase from midguts of larvae of the bruchid beetle *Callosobruchus maculatus* (F.). Comp Biochem Physiol 92B:55–57.

Yamasaki Y. 2003. β-Amylase in germinating millet seeds. Phytochemistry 64:935–939.

Yang S-J, Lee H-S, Park C-S, Kim Y-R, Moon T-W, Park K-H. 2004. Enzymatic analysis of an amylolytic enzyme from the hyperthermophilic archaeon *Pyrococcus furiosus* reveals its novel catalytic properties as both an α-amylase and a cyclodextrin-hydrolyzing enzyme. Appl Environ Microbiol 70:5988–5995.